

Renormalization Group Solution of the Chutes&Ladder Model

Lauren A. Ball, Alfred C. K. Farris, and Stefan Boettcher*
Dept. of Physics, Emory University, Atlanta, GA 30322; USA

We analyze a semi-infinite one-dimensional random walk process with a biased motion that is incremental in one direction and long-range in the other. On a network with a fixed hierarchy of long-range jumps, we find with exact renormalization group calculations that there is a dynamical transition between a localized adsorption phase and an anomalous diffusion phase in which the mean-square displacement exponent depends non-universally on the Bernoulli coin. We relate these results to similar findings of unconventional phase behavior in hierarchical networks.

I. INTRODUCTION

The variety of real networks found in biology, engineering, social sciences, and communication provides a need for new ideas to explore and classify the full range of critical phenomena that emerge as a result of the complex geometry [1–4]. Networks with a hierarchical organization of its sites have a long history in providing solvable models of statistical systems [5, 6]. More recently, such networks, when turned hyperbolic with the addition of small-world links, have received considerable attention due to a variety of synthetic phase transitions that can be observed in such structures for well-known equilibrium models such as percolation [7–9] and Ising ferromagnets [10–14]. For instance, hyperbolic networks interwoven with geometric backbones provide solvable examples of discontinuous (“explosive”) percolation transitions [15–17]. Previous studies of symmetric walks on such networks give simple examples of super-diffusion and shown close connections with Lévy flights [18, 19].

Here, we consider a strongly biased variant of the familiar persistent random walk [20, 21]; an incrementally progressing walker in the forward direction undertakes back-jumps with a tunable frequency that is inversely related to the length of the long jump. But unlike those persistent walks that typically remain within the universality class of ordinary diffusion [21], the asymptotic behavior of our walks exhibit anomalous diffusion behavior with exponents that depend on the long-jump bias of the Bernoulli coin p . For instance, for the exponent that relates typical length and time-scales, $T \sim L^{d_w}$, such as determined through the mean-square displacement, we find

$$d_w(p) = \log_2 \left(\frac{2 - 3p}{1 - 2p} \right), \quad (1)$$

which continuously ranges through $0 < p \leq \frac{1}{2}$, from straight ballistic motion, $d_w(0) = 1$, to all forms of anomalous super and sub-diffusion down to complete confinement or adsorption [22], $d_w = \infty$, for $p > \frac{1}{2}$. For instance, according to Eq. (1), exactly at $p = \frac{1}{5}$ the balance between step-by-step progression and occasional fall-backs results in an effectively diffusive spreading, $d_w = 2$, at long ranges. Among other benefits, the

tunability of the spreading walk provides strong control over transport properties[23, 24] as well as mixing times. Combined with some forms of control, persistent walks such as this, for example, have received some renewed attention recently as a means to accelerate Markov chain algorithms via “lifting” [25–27]. Furthermore, quantized version of such walks are a fundamental ingredient in quantum algorithms [28–30].

First and foremost, our study here serves as a simple illustration of the unusual – and often non-universal – scaling behavior for dynamic processes on complex networks. In particular, hyperbolic networks such as the one considered here have been shown to possess a number of interesting, *synthetic* phase transitions in which the scaling behavior can be controlled by global parameters [11, 31, 32]. However, our model also provides a sense of what might happen in an ordinary, one-dimensional lattice with an incremental bias to walk one direction and back-jumps in the opposite direction, drawn randomly (annealed) from a Lévy-flight distribution [33]. This could be extended, for example, to model the behavior of directional transport of kinesin [34], interrupted with finite failure rate that leads to dissociation off the actin filament to reset the process. Certain forms of foraging behavior have also been described in these terms [35–38].

Our discussion is organized as follows. In the next section, we describe the network we are using and the random walk on it. In Sec. IV, we describe the results of our numerical simulations. In Sec. V we discuss our renormalization group calculation. Finally, we conclude our discussion in Sec. VI.

II. NETWORK DESIGN

The network we are discussing in this paper [39] consists of a simple geometric backbone, a one-dimensional line of $N = 2^l$ sites ($0 \leq n \leq 2^l$, $l \rightarrow \infty$). Each site on the one-dimensional lattice backbone is connected to its nearest neighbor. To generate the small-world hierarchy in these graphs, consider parameterizing any integer n (except for zero) *uniquely* in terms of two other integers

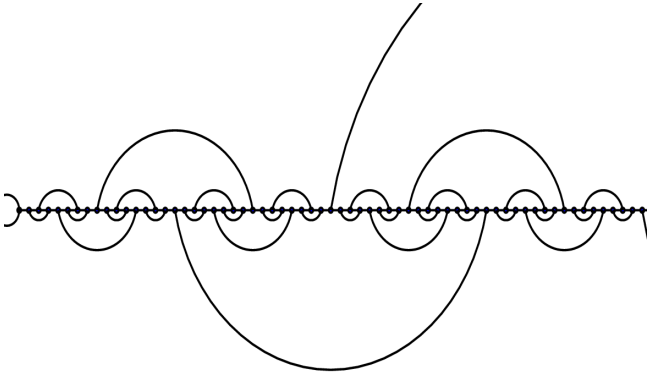


Figure 1. Depiction of HN3 on a semi-infinite line. The leftmost site here is $n = 0$, which requires special treatment.

(i, j) , $i \geq 0$,

$$n = 2^i (2j + 1). \quad (2)$$

Here, i denotes the level in the hierarchy whereas j labels consecutive sites within each hierarchy. For instance, $i = 0$ refers to all odd integers, $i = 1$ to all integers once divisible by 2 (i. e., 2, 6, 10,...), and so on. In these networks, aside from the backbone, each site is also connected with (one or both) of its nearest neighbors *within* the hierarchy. We obtain the 3-regular network HN3 by connecting first all nearest neighbors along the backbone, but in addition also 1 to 3, 5 to 7, 9 to 11, etc, for $i = 0$, next 2 to 6, 10 to 14, etc, for $i = 1$, and 4 to 12, 20 to 28, etc, for $i = 2$, and so on, as depicted in Fig. 1. The site with index zero, not being covered by Eq. (2), is clearly a special place on the boundary of the HN3 that provides an impenetrable wall and ensures that the walks remains semi-infinite.

III. CHUTES & LADDER MODEL

We will study biased random walks on HN3. Each site of HN3 has degree three, i.e., the walker has three possible ways to exit her current position, as indicated in Fig. 2: up or down the backbone, or along the long-range link. The option with a walk that is unbiased for hops along the backbone has been studied in Refs. [18, 19]. Here, we consider the extreme case of a walker that can move along the backbone in only one direction (“up”) while along the small-world links it can only move in the opposite direction (“down”). At a site at which the long-range link is oriented in the up-direction, the walker *deterministically* moves up along the backbone. Only at sites with a long-range link in the down-direction does the walker have a choice. Thus, all walks are controlled by the parameter p , the Bernoulli coin, which is the probability of a walker to jump off the lattice in a long-range jump down towards the origin. At such a site, the walker will move

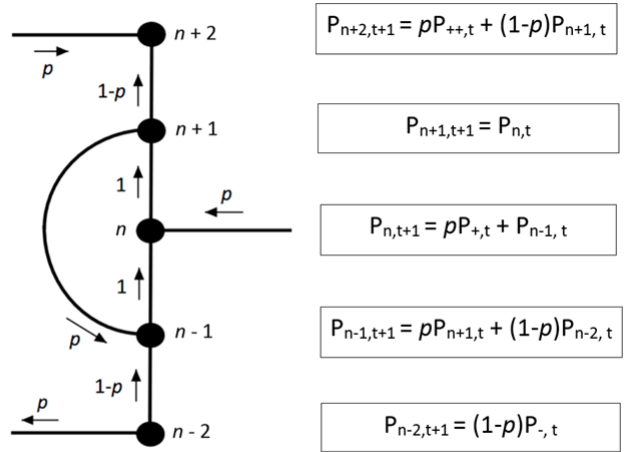


Figure 2. Hopping probabilities between sites in the typical sub-graph of HN3, the network depicted in Fig. 1. Shown are the hopping probabilities from each site at time t , and the corresponding equations describing the probability of the site being occupied at time $t + 1$. (Subscripts “+”, “++”, and “-” refer to unspecified distant sites connected via long-range jumps.)

up along the backbone with probability $(1 - p)$. These probabilities are displayed in Fig. 2. If p were set to zero, we would obtain a ballistic one-dimensional walk, exclusively biased in the up-direction. For any finite p , the walk resembles the popular children’s game of “Chutes & Ladders” [40].

IV. NUMERICAL SIMULATIONS

In our simulations, each walk begins at site $n = 1$ at time $t = 0$. This excludes site $n = 0$ from the process, as it can not be reached. It results in a semi-infinite walk restricted to all sites of positive index n . Having arrived at any site n , the procedure for determining the walker’s next step involves first calculating each path that he could potentially take from its current position, based on the HN3 geometry. First, we determine the level in the hierarchy of the possible long-range jump, i in Eq. (2), by counting how many times the current site index n is divisible by two. After peeling this factor of 2^i off n , we obtain $n/2^i = 2j + 1$, an odd number. If now j is also an odd number, the walker is located at a long-range link in the down-direction; if instead j is even, the long-range link emanating from n is oriented in the up-direction and blocked for the walker. In the latter case, the walker must move up by one step along the backbone. In the former case, it has two possibilities: with probability p the long-range link in the down-direction is taken, while with probability $1 - p$ the walker will move up along the backbone.

We have conducted extensive sampling of such a walk for each value of $p = 0.1, 0.2, \dots, 0.9$ by averaging the mean-square displacement (MSD) as a function of time over at least 10^6 walks that were terminated after $t_{\max} = 2^{27} \approx 10^8$ update steps. In the expectation of an anomalous power-law relation of the MSD with time,

$$\langle r^2 \rangle \sim D t^{\frac{2}{d_w}} \quad (3)$$

with some positive constant D , in Fig. 3(a) we have plotted our data in the form of an extrapolation plot,

$$\frac{\ln \langle r^2 \rangle}{2 \ln t} \sim \frac{1}{d_w} + \frac{\ln D}{\ln t}. \quad (4)$$

When plotted on an $1/\ln t$ -scale as the x -axis, the data should extrapolate *linearly* to the desired MSD exponent, $1/d_w$, read off on the intercept with the y -axis for $t \rightarrow \infty$. In the figure, we have marked those intercepts with blue stars for each value of p . In Fig. 3(b) we plot those extrapolants as a function of p . In that panel, we have also indicated the exact RG-result advertised in Eq. (1) as a solid line. Our data matches that line within errors for all $p < \frac{1}{2}$, while for values of $p \geq \frac{1}{2}$, where the walk develops a strong bias towards returning to the origin (i.e., $d_w \rightarrow \infty$), there are strong deviations due to slow convergence and, for $p > \frac{1}{2}$, a break-down of the power-law assumption (i.e., a lack of a linear extrapolation) in Eq. (3), as is also apparent from the break-down of Eq. (1) for $p > \frac{1}{2}$. In that regime, the walker remains entirely confined near the origin.

The failure of our extrapolation near $p = \frac{1}{2}$ is easy to understand: For $p \nearrow \frac{1}{2}$, $d_w \sim \log_2(\frac{1}{2} - p)$ diverges rapidly, and at $1/d_w \approx 0.1$, say, after t_{\max} updates a walker has typically only explored at most $l_{\max} \approx (10^8)^{0.1} \lesssim 10$ sites from the origin; far too small a range to approximate asymptotic scaling, especially in a heterogeneous structure such as HN3.

V. RENORMALIZATION GROUP ANALYSIS

To develop the renormalization group analysis for this problem, we start from the master equation for the probability to be at site n after t update steps, $P_{n,t}$ [41]. In Fig. 2, we show an example set of recursions for some 5-site segment of HN3. These on-site probabilities at subsequent times depend in delicate ways on the inflow of probability from neighboring sites via the specific local structure of incoming and outgoing long-rang links that can vary a lot from segment to segment.

In order to have a finite set of closed equations to obtain a closed set of RG-recursions for hopping parameters, we study a sequence of finite-sized systems with $N_l = 2^l$ sites for $l = 2, 3, \dots$. For each, we use a generat-

ing function,

$$\tilde{P}_n(z) = \sum_{t=0}^{\infty} P_{n,t} z^t, \quad (5)$$

in order to eliminate time dependence with this Laplace transform. For the resulting hierarchy of ordinary recursion for a given l , we then trace out every second site amplitude \tilde{P}_n , those for odd values of n , by algebraic means. This obtains a new such hierarchy in a form corresponding to a system corresponding to $l-1$ but with more complex hopping parameters. We repeat this procedure until we discover a closed set of recursions amongst the hopping parameters.

Here we demonstrate the RG process used to determine the recursion equations by starting on a 16-site network ($l = 4$) depicted in Fig. 4 and renormalizing it to an 8-site network ($l = 3$), revealing a self-similar pattern amongst the hopping parameters. First, we rewrite the generic master equations, $P_{n,t+1} = \sum_m U_{n,m} P_{m,t}$, as $\tilde{P}_n = z \sum_m U_{n,m} \tilde{P}_m$ by applying Eq. (5), for some evolution matrix $U_{n,m}$ that describes the hopping between sites. For the specific choice of $U_{n,m}$ referring to the structure shown in Fig. 4, we reach the following hierarchy of equations in terms of z and p :

$$\begin{aligned} \tilde{P}_0 &= 1, \\ \tilde{P}_1 &= z\tilde{P}_0 + zp\tilde{P}_3, \\ \tilde{P}_2 &= z\tilde{P}_1 + zp\tilde{P}_6, \\ \tilde{P}_3 &= z\tilde{P}_2, \\ \tilde{P}_4 &= z(1-p)\tilde{P}_3 + zp\tilde{P}_{12}, \\ \tilde{P}_5 &= z\tilde{P}_4 + zp\tilde{P}_7, \\ \tilde{P}_6 &= z\tilde{P}_5, \\ \tilde{P}_7 &= z(1-p)\tilde{P}_6, \\ \tilde{P}_8 &= z(1-p)\tilde{P}_7 + zp\tilde{P}_{16}, \\ \tilde{P}_9 &= z\tilde{P}_8 + zp\tilde{P}_{11}, \\ \tilde{P}_{10} &= z\tilde{P}_9 + zp\tilde{P}_{14}, \\ \tilde{P}_{11} &= z\tilde{P}_{10}, \\ \tilde{P}_{12} &= z(1-p)\tilde{P}_{11}, \\ \tilde{P}_{13} &= z(1-p)\tilde{P}_{12} + zp\tilde{P}_{15}, \\ \tilde{P}_{14} &= z\tilde{P}_{13}, \\ \tilde{P}_{15} &= z(1-p)\tilde{P}_{14}, \\ \tilde{P}_{16} &= z(1-p)\tilde{P}_{15}. \end{aligned} \quad (6)$$

Here, we choose to terminate the lattice by connecting the 8th site to the 16th site, instead of the 24th site as it would have otherwise been by the rules of construction of the network in Sec. II. This small change does not affect the asymptotic behavior of the system at large sizes and times for observables such as the MSD.

After some trial-and-error, starting with a larger set of generalized hopping parameters, we arrive at a minimal

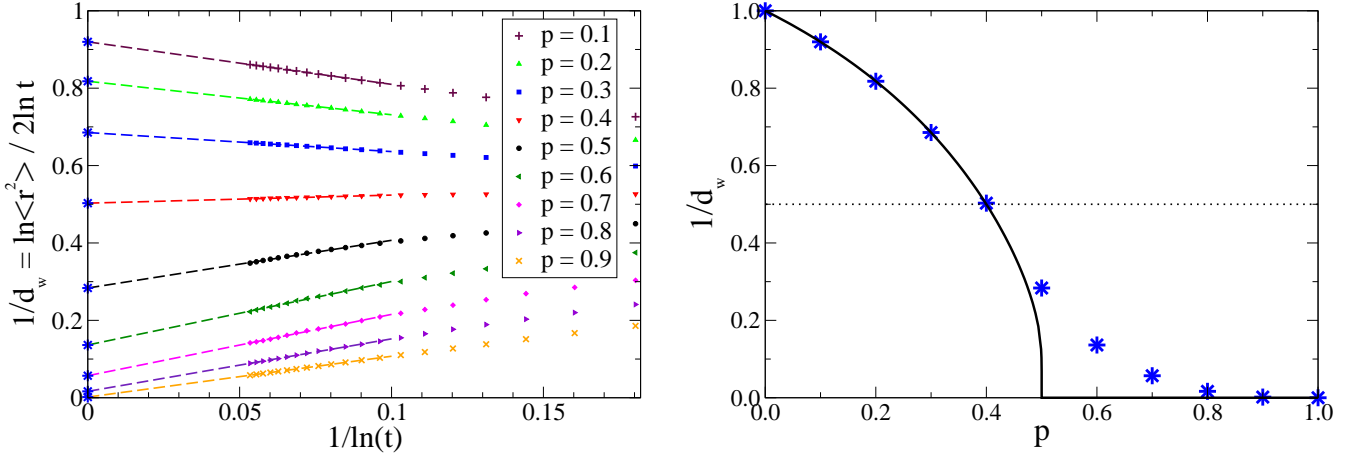


Figure 3. (a) Extrapolation of the data obtained for the mean-square displacement for the walk at different values of the down-jump probability p from simulations run up to a temporal cutoff at $t = 2^{27}$. We used a linear fit according to Eq. (4) to the data set for each value of p deep in the asymptotic regime for large t , as indicated by the fitted lines, data for all smaller t were ignored. While statistical errors are much below the symbol size, large corrections to linear behavior are apparent for larger p , suggesting large systematic errors. The fitted values for $1/d_w$ of the extrapolation for $t \rightarrow \infty$ are marked as blue stars at the intercept. (b) These extrapolated values (blue stars) for the exponent d_w found are plotted as a function of p . The solid line corresponds to the exact RG-result according to Eq. (1).

set necessary to parameterize Eq. (6) such that a closed system of RG-recursions is obtained between those parameters. Inserting these parameters in Eqs. (6) yields

$$\begin{aligned}
 \tilde{P}_0 &= 1 \\
 \tilde{P}_1 &= a\tilde{P}_0 + b\tilde{P}_3, \\
 \tilde{P}_2 &= c\tilde{P}_1 + d\tilde{P}_6, \\
 \tilde{P}_3 &= g\tilde{P}_2, \\
 \tilde{P}_4 &= e\tilde{P}_3 + d\tilde{P}_{12}, \\
 \tilde{P}_5 &= a\tilde{P}_4 + b\tilde{P}_7, \\
 \tilde{P}_6 &= c\tilde{P}_5, \\
 \tilde{P}_7 &= f\tilde{P}_6, \\
 \tilde{P}_8 &= e\tilde{P}_7 + d\tilde{P}_{16}, \\
 \tilde{P}_9 &= a\tilde{P}_8 + b\tilde{P}_{11}, \\
 \tilde{P}_{10} &= c\tilde{P}_9 + d\tilde{P}_{14}, \\
 \tilde{P}_{11} &= g\tilde{P}_{10}, \\
 \tilde{P}_{12} &= e\tilde{P}_{11}, \\
 \tilde{P}_{13} &= k\tilde{P}_{12} + b\tilde{P}_{15}, \\
 \tilde{P}_{14} &= c\tilde{P}_{13}, \\
 \tilde{P}_{15} &= f\tilde{P}_{14}, \\
 \tilde{P}_{16} &= e\tilde{P}_{15},
 \end{aligned} \tag{7}$$

where we can read off the initial conditions from Eqs. (6) for these generalized hopping parameters at RG-step

$l = 0$:

$$\begin{aligned}
 a_0 &= z, & b_0 &= zp, & c_0 &= z, \\
 d_0 &= zp, & e_0 &= z(1-p), & f_0 &= z(1-p), \\
 g_0 &= z, & k_0 &= z(1-p).
 \end{aligned} \tag{8}$$

The parameters used in this system of equations are depicted in Fig. 4.

A single step of the RG involves solving the hierarchy in Eq. (7) for \tilde{P}_n with odd values of n , and then eliminating them from every other equation, leaving equations that only contain amplitudes with even n :

$$\begin{aligned}
 \tilde{P}_0 &= 1, \\
 \tilde{P}_2 &= \frac{ac}{1-bcg} \tilde{P}_0 + \frac{d}{1-bcg} \tilde{P}_6, \\
 \tilde{P}_4 &= eg \tilde{P}_2 + d \tilde{P}_{12}, \\
 \tilde{P}_6 &= \frac{ac}{1-bcf} \tilde{P}_4, \\
 \tilde{P}_8 &= ef \tilde{P}_6 + d \tilde{P}_{16}, \\
 \tilde{P}_{10} &= \frac{ac}{1-bcg} \tilde{P}_8 + \frac{d}{1-bcg} \tilde{P}_{14}, \\
 \tilde{P}_{12} &= eg \tilde{P}_{10}, \\
 \tilde{P}_{14} &= \frac{ck}{1-bcf} \tilde{P}_{12}, \\
 \tilde{P}_{16} &= ef \tilde{P}_{14}.
 \end{aligned} \tag{9}$$

Comparing the coefficients of these equations originating at the previous RG-step to the corresponding coefficients

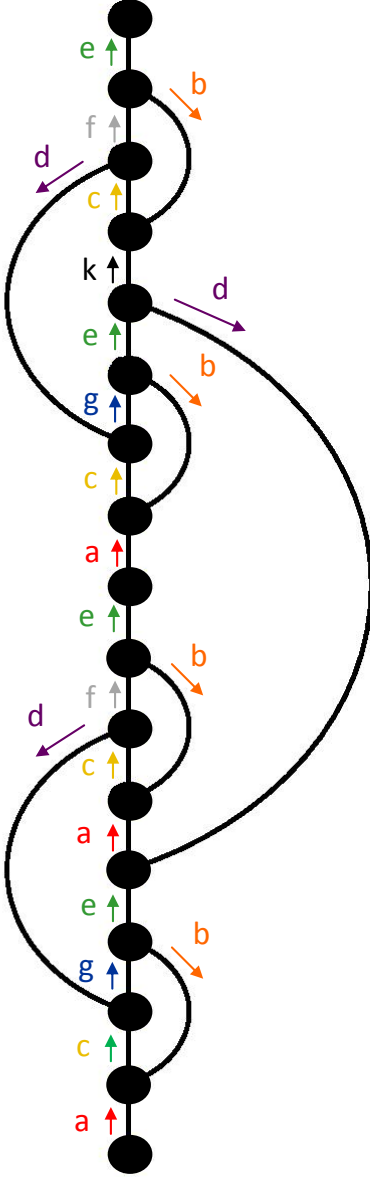


Figure 4. Definition of renormalizable hopping parameters for the biased walk along HN3. During each RG-step, every second site is eliminated algebraically and a new set of equations result which are identical in form to the previous set. Comparing the hopping parameters in these equations before and after each step leads to the RG-flow in Eq. (10).

describing the RG-flow of the system:

$$\begin{aligned}
 a_{l+1} &= \frac{a_l c_l}{1 - b_l c_l g_l}, \\
 b_{l+1} &= \frac{z p}{1 - b_l c_l g_l}, \\
 c_{l+1} &= e_l g_l, \\
 e_{l+1} &= e_l f_l, \\
 f_{l+1} &= \frac{k_l c_l}{1 - b_l c_l f_l}, \\
 g_{l+1} &= \frac{a_l c_l}{1 - b_l c_l f_l}, \\
 k_{l+1} &= \frac{k_l c_l}{1 - b_l c_l g_l}.
 \end{aligned} \tag{10}$$

The RG-flow in Eqs. (10) describe how the generalized hopping parameters transform under rescaling the system size from N to $2N$. At this point, we can further simplify these recursions. First, note that there is no equation for the flow of the parameter d — it maintains its initial value $d_l = d_0 = zp$ throughout. In this way, the RG-flow remains explicitly dependent on the microscopic probability p , which will lead to the non-universality of the MSD exponent in Eq. (1). This explicit dependence of the RG-flow on the control parameter is typical for hyperbolic networks that leads to a number of novel critical phenomena [10, 11, 15, 31] in equilibrium thermodynamics. Secondly, we observe that the recursions for a_l and k_l , and consequently also for f_l and g_l as well as e_l and c_l , are identical, with the distinction between each pair merely due to their difference in the initial conditions in Eqs. (8). However, setting throughout $k_l = (1 - p) a_l$, $f_l = (1 - p) g_l$, and $e_l = (1 - p) c_l$, which clearly reflects their corresponding yet asymmetric roles at opposite ends of a long-range jump in Fig. 4, leads to a much reduced set of equations:

$$\begin{aligned}
 a_{l+1} &= \frac{a_l c_l}{1 - b_l c_l g_l}, \\
 b_{l+1} &= \frac{z p}{1 - b_l c_l g_l}, \\
 c_{l+1} &= (1 - p) c_l g_l, \\
 g_{l+1} &= \frac{a_l c_l}{1 - (1 - p) b_l c_l g_l},
 \end{aligned} \tag{11}$$

To verify the closure of the RG-flow, we consider a system of 64 sites and confirm that the recursions maintain their self-similarity at each RG-step. We conclude that the four distinct parameters given in Eq. (11) are complete to describe the behavior of the system [41].

We note that this system of non-linear recursions, in fact, has exact solutions for the case that $z = 1$. Evolving the recursions from the initial conditions, we find the relations $a_l c_l \equiv 1$ and $b_l \equiv p a_l$ to persist for all l . With that Ansatz, we can reduce the system to a single recursion,

$$g_{l+1} = \frac{1}{1 - p(1 - p)g_l}, \tag{12}$$

of Eqs. (7) at the next RG-step gives us the recursions

which is similar to those found for continued fractions [42]. It has the solution,

$$g_l = \frac{\left(\frac{1-p}{p}\right)^{l+1} - 1}{p \left[\left(\frac{1-p}{p}\right)^{l+2} - 1\right]}, \quad (13)$$

for $g_0 = 1$, from which the solutions for the other parameters easily follows. Unfortunately, this solution can not be easily extended to values of $z < 1$.

We now restrict our study to the fixed point (FP) of the RG-flow in Eqs. (11) that describes the asymptotic properties of the walk: For asymptotically large systems $l \rightarrow \infty$ we look for stationary solutions setting $l \sim l + 1$ to get

$$\begin{aligned} a_\infty &= \frac{1 - pz}{1 - (1 + z)p}, \\ b_\infty &= \frac{(1 - p)pz}{1 - (1 + z)p}, \\ c_\infty &= \frac{1 - (1 + z)p}{1 - p}, \\ g_\infty &= \frac{1}{1 - p}. \end{aligned} \quad (14)$$

To characterize the dynamics of the system in the limit of large systems at long times, we endeavor to study the simultaneous limits of $l \rightarrow \infty$ and $\epsilon = 1 - z \rightarrow 0$, to which end we linearize in ϵ the RG-flow in Eqs. (11) near the fixed point. We do this by taking the Jacobian J of these recursion equations, which is the matrix consisting of the first-order derivatives of each recursion equations with respect to each independent hopping parameter,

$$J_l = \begin{pmatrix} \frac{c}{1-bcg} & \frac{ac^2g}{(1-bcg)^2} & \frac{a}{(1-bcg)^2} & \frac{abc^2}{(1-bcg)^2} \\ 0 & \frac{pcg}{(1-bcg)^2} & \frac{pbg}{(1-bcg)^2} & \frac{pbc}{(1-bcg)^2} \\ 0 & 0 & (1-p)g & (1-p)c \\ \frac{c}{1-(1-p)bcg} & \frac{(1-p)ac^2g}{[1-(1-p)bcg]^2} & \frac{a}{[1-(1-p)bcg]^2} & \frac{(1-p)abc^2}{[1-(1-p)bcg]^2} \end{pmatrix}, \quad (15)$$

which evaluated at the fixed point in Eqs. (14) gives:

$$J_\infty = \begin{pmatrix} 1 & \frac{1}{1-2p} & \frac{(1-p)^3}{(1-2p)^3} & \frac{p(1-p)^2}{(1-2p)^2} \\ 0 & \frac{p}{1-2p} & \frac{(1-p)^2p^2}{(1-2p)^3} & \frac{(1-p)^2p^2}{(1-2p)^2} \\ 0 & 0 & 1 & 1-2p \\ \frac{1-2p}{(1-p)^2} & \frac{1-2p}{(1-p)^3} & \frac{1}{(1-p)(1-2p)} & \frac{p}{1-p} \end{pmatrix}. \quad (16)$$

Since by Eq. (5) it is $z^t \sim e^{-\epsilon t}$, the largest eigenvalue λ of the Jacobian J_∞ describes the rescaling of time, $T \rightarrow T' = \lambda T$ under rescaling space, $L \rightarrow L' = 2L$, during the RG-step $l \rightarrow l + 1$. The largest eigenvalue of J_∞ in Eq. (16) is

$$\lambda = \frac{2 - 3p}{1 - 2p}. \quad (17)$$

The scaling Ansatz for the similarity scaling relation between time and space, $T \sim L^{d_w}$, yields $d_w = \log_2 \lambda$, for which the eigenvalue in Eq. (17) finally gives Eq. (1).

VI. CONCLUSIONS

We have presented a simple and exactly solvable example of a complex (hyperbolic) network for which a biased random walk leads to a non-universal scaling behavior in which scaling exponents remain dependent on the control parameter p for the strength of the bias for $0 \leq p \leq \frac{1}{2}$. For $p > \frac{1}{2}$, the walker will stay confined near the origin, because long-range jumps backwards along the network will be taken frequently. Our analytical result, obtained via a renormalization group calculation, are consistent with our numerical simulations for $p < \frac{1}{2}$, and the scaling Ansatz fails for the data at $p > \frac{1}{2}$, consistent with the exact result again. The origin of the non-universality that is introduced through the non-renormalization of long-range links, is reminiscent of similar findings for these hyperbolic networks in equilibrium critical phenomena where they lead to novel synthetic phase transitions that allow a high-level of engineering control [15]. While easy to engineer, critical phenomena on such hierarchical structures tend to be very fragile to any form of disorder, however, which is an issue that should be analyzed in more detail in the future.

ACKNOWLEDGEMENTS

LAB thanks the Clare Boothe Luce Foundation for a fellowship. SB acknowledges financial support from the U. S. National Science Foundation through grant DMR-1207431.

* sboettc@emory.edu; <http://www.physics.emory.edu/faculty/boettcher/>

- [1] A.-L. Barabasi, *Linked: How Everything Is Connected to Everything Else and What It Means for Business, Science, and Everyday Life* (Plume Books, 2003).
- [2] S. Boccaletti, V. Latora, Y. Moreno, M. Chavez, and D.-U. Hwang, Phys. Rep. **424**, 175 (2006).
- [3] S. N. Dorogovtsev, A. V. Goltsev, and J. F. F. Mendes, Rev. Mod. Phys. **80**, 1275 (2008).
- [4] M. Barthélemy, Physics Reports **499**, 1 (2011).
- [5] D. Dhar, J. Math. Phys. **18**, 578 (1977).
- [6] A. N. Berker and S. Ostlund, Journal of Physics C: Solid State Physics **12**, 4961 (1979).
- [7] A. N. Berker, M. Hinczewski, and R. R. Netz, Phys. Rev. E **80**, 041118 (2009).
- [8] S. Boettcher, J. L. Cook, and R. M. Ziff, Phys. Rev. E **80**, 041115 (2009).
- [9] T. Hasegawa, T. Nogawa, and K. Nemoto, EuroPhys. Lett. **104**, 16006 (2013).

- [10] T. Nogawa, T. Hasegawa, and K. Nemoto, *Phys. Rev. Lett.* **108**, 255703 (2012).
- [11] S. Boettcher and C. T. Brunson, *Phys. Rev. E* **83**, 021103 (2011).
- [12] R. F. S. Andrade, J. J. S. Andrade, and H. J. Herrmann, *Phys. Rev. E* **79**, 036105 (2009).
- [13] M. Hinczewski and A. N. Berker, *Phys. Rev. E* **73**, 066126 (2006).
- [14] M. Hinczewski, *Physical Review E* **75**, 061104 (2007).
- [15] S. Boettcher, V. Singh, and R. M. Ziff, *Nature Communications* **3**, 787 (2012).
- [16] V. Singh and S. Boettcher, *Physical Review E* **90**, 012117 (2014).
- [17] Y. S. Cho and B. Kahng, (arXiv:1404.4470).
- [18] S. Boettcher and B. Gonçalves, *Europhysics Letters* **84**, 30002 (2008).
- [19] S. Boettcher, B. Gonçalves, and J. Azaret, *Journal of Physics A: Mathematical and Theoretical* **41**, 335003 (2008).
- [20] A. Chen and E. Renshaw, *Journal of Applied Probability* **31**, pp. 869 (1994).
- [21] G. H. Weiss, *Aspects and Applications of the Random Walk* (North-Holland, Amsterdam, 1994).
- [22] S. Boettcher and M. Moshe, *Phys. Rev. Lett.* **74**, 2410 (1995).
- [23] J. Otwinowski and S. Boettcher, *J. Stat. Mech.* **P07010** (2009).
- [24] S. Boettcher, C. Varghese, and M. A. Novotny, *Phys. Rev. E* **83**, 041106 (2011).
- [25] F. Chen, L. Lovasz, and I. Pak, in *Proc. 17th Annual ACM Symposium on Theory of Computing* (1999) pp. 275–281.
- [26] T. P. Hayes and A. Sinclair, *Lecture Notes in Computer Science* **6302**, 602 (2010).
- [27] Y. Sakai and K. Hukushima, *Journal of the Physical Society of Japan* **82**, 064003 (2013).
- [28] L. K. Grover, *Phys. Rev. Lett.* **79**, 325 (1997).
- [29] D. Aharonov, A. Ambainis, J. Kempe, and U. Vazirani, in *Proc. 33rd Annual ACM Symp. on Theory of Computing (STOC 2001)* (ACM, New York, NY, 2001) pp. 50–59.
- [30] S. Boettcher, S. Falkner, and R. Portugal, *Journal of Physics: Conference Series* **473**, 012018 (2013).
- [31] S. Boettcher and C. T. Brunson, (arXiv:1209.3447).
- [32] V. Singh, C. T. Brunson, and S. Boettcher, (arXiv:1408.0669).
- [33] M. F. Shlesinger, G. M. Zaslavsky, and J. Klafter, *Nature* **363**, 31 (1993).
- [34] K. C. Huang, C. Vega, and A. Gopinathan, *Journal of Physics: Condensed Matter* **23**, 374106 (2011).
- [35] G. M. Viswanathan, S. V. Buldyrev, S. Havlin, M. G. E. da Luz, E. P. Raposo, and H. E. Stanley, *Nature* **401**, 911 (1999).
- [36] C. L. Faustino, L. R. da Silva, M. G. E. da Luz, E. P. Raposo, and G. M. Viswanathan, *EPL (Europhysics Letters)* **77**, 30002 (2007).
- [37] P. J. Ribeiro-Neto, E. P. Raposo, H. A. Araújo, C. L. Faustino, M. G. E. da Luz, and G. M. Viswanathan, *Phys. Rev. E* **86**, 061102 (2012).
- [38] C. L. Faustino, M. L. Lyra, E. P. Raposo, G. M. Viswanathan, and M. G. E. da Luz, *EPL (Europhysics Letters)* **97**, 50005 (2012).
- [39] S. Boettcher, B. Gonçalves, and H. Guclu, *J. Phys. A: Math. Theor.* **41**, 252001 (2008).
- [40] [Http://uncyclopedia.wikia.com/wiki/Chutes_and_Ladders](http://uncyclopedia.wikia.com/wiki/Chutes_and_Ladders).
- [41] S. Redner, *A Guide to First-Passage Processes* (Cambridge University Press, Cambridge, 2001).
- [42] C. M. Bender and S. A. Orszag, *Advanced Mathematical Methods for Scientists and Engineers* (McGraw-Hill, New York, 1978).